Test structure and measurement system for characterising the electrochemical performance of nanoelectrode structures

Ilka Schmueser[1,2], Ewen O. Blair[1,2,*], Ziya Isiksacan[1,*], Yifan Li[1,*], Damion K. Corrigan[2,*], Adam A. Stokes[1], Jonathan G. Terry[1], Andrew R. Mount[2] and Anthony J. Walton[1]
[1]School of Engineering, The University of Edinburgh, Edinburgh, UK
[2]School of Chemistry, The University of Edinburgh, Edinburgh, UK
Email: I.Schmueser@ed.ac.uk

***Abstract*—This paper presents a complete test structure and characterisation system for the evaluation of nanoelectrode technology. It integrates microfabricated nanoelectrodes for electrochemical measurements, 3D printing and surface tension-confined microfluidics. This system exploits the inherent analytical advantages of nanoelectrodes that enables their operation with small volume samples, which has potential applications for on-wafer measurements.**

I. Introduction

Nanoelectrode arrays have been an area of considerable interest in electrochemical research for many decades [1-3]. Reduction of electrode dimension from macro through micro to nano delivers enhanced sensing properties such as higher signal to noise ratio, lower limit of detection, reduced susceptibility to convection, faster response times, and, in some configurations, a time-independent steady state signal [4]. This results from the radial diffusion characteristics of smaller electrodes compared to the nearly exclusively planar diffusion found for larger electrodes. Commonly, the transition between macro and microelectrodes is observed at a critical dimension of around 50 µm and with further reduction of this dimension, these properties are further enhanced as transport becomes progressively more efficient.

This paper describes a nanoelectrode array test structure together with a full characterization system. In its final implementation, such a test structure would be probed at wafer-level, therefore presenting a challenge for a sensor which requires contact with liquid without evaporation [5]. A potential solution could be a confined, thin film of liquid over the surface, which not only prevents evaporation but is more uniform than a droplet. To simulate this, a 3D printed jig is used in combination with surface tension controlled microfluidics to corral a thin liquid film over the test structure and asses its performance. The novelty of the proposed approach arises from the integration of a number of technologies:

- microfabrication used to fabricate the test structure wafer with three electrochemical electrodes, including the nanoarray working electrode, and the surface tension controlling surfaces
- surface tension controlled microfluidics in a parallel plate arrangement to corral the liquid sample on the wafer surface atop the electrodes
- 3D printing for the fabrication of the cell assembling the separate components.

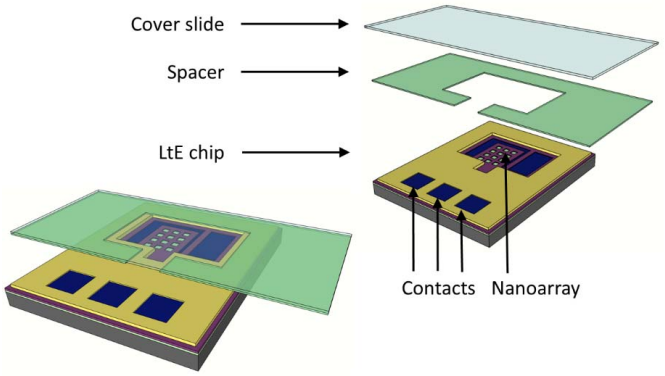

Fig. 1. A schematic 3D view of electrodes and cover-glass (note the cavities containing the nanoelectrodes in this figure are considerably larger and less numerous for illustration purposes).

The individual components are first summarized and then their integration to create the system is described. This is then benchmarked against an identical measurement in a beaker to demonstrate its capability to perform electrochemical measurements to the same, if not better, standard. A schematic of the major elements of the test structure and the characterization system is shown in Fig. 1.

II. System Design and Fabrication

A. Overall Design Concept

For this test structure, hydrophilic and hydrophobic surfaces are used to corral the sample liquid of microliter volume

[*] E.O.B. and D.K.C. are now at Faculty of Engineering, University of Strathclyde, Glasgow, UK; Y.L. is now at Department of Mechanical and Construction Engineering, Northumbria University, Newcastle, UK; Z.I. is now at UNAM Institute of Materials Science and Nanotechnology, Bilkent University, Ankara, Turkey

978-1-7281-4008-7/20 $31.00 © 2020 IEEE

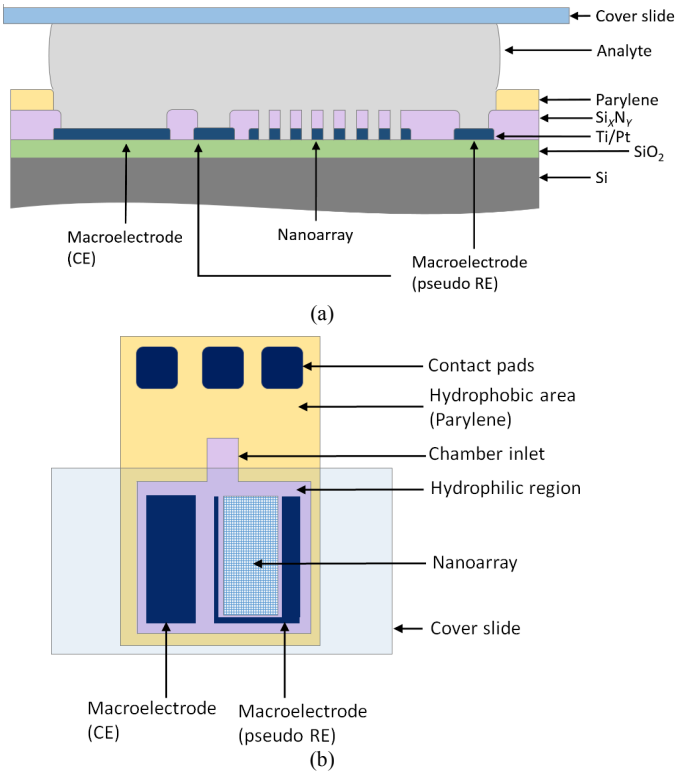

Fig. 2. (a) A schematic cross-section and (b) top view of the cell (note not to scale).

between the chip and a parallel glass plate separated using either features in the 3D printed cell, or a spacer sheet. Fig. 2 shows (a) a cross-section of the resulting cell and (b) a schematic layout detailing the two plates. In this test structure design, the chip substrate is silicon and the layout includes the electrodes, electrical contacts and interconnects, as well as the hydrophobic regions that confine the aqueous electrolyte. Fig. 3(a) and (b) show images demonstrating that liquid is successfully corralled by the virtual walls created between the hydrophobic and hydrophilic regions for systems where the 3D printed jig and a spacer sheet are used to set the liquid height, respectively. The use of the invisible wall technology considerably simplifies cell construction and avoids any potential leakage or contamination issues associated with gasket seals, channel bonding and/or reservoirs. Combining this with a glass plate set at a defined distance parallel to the substrate ensures a uniform thickness of electrolyte, which simplifies configuration, response and analysis and enables the measurements of very small sample volumes.

B. *Nanoelectrode Array Working, Counter and Reference Electrodes*

The employment of nanoelectrode arrays as the working electrode (WE) most importantly facilitates the ability to analyze small sample volumes and creates the enhanced sensors response detailed previously. Briefly, the electrodes employed in this work as the test structures are vertical platinum bands of defined nanometer-scale thickness, sandwiched between two insulation layers. They are formed at the perimeter of the defined micrometer sized cavities in an array by etching (see Fig. 2(a)). The reference electrode (RE) provides a pseudo reference

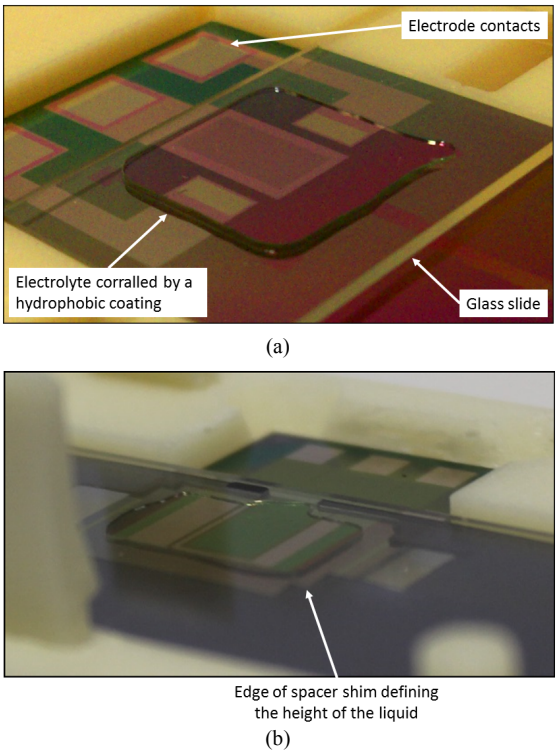

Fig. 3. Examples of liquid filled electrochemical cells using a hydrophobic coating to corral the electrolyte sandwiched between the silicon electrode substrate and a cover-glass showing (a) An electrode designed for when the height is set to a fixed value by the jig (225 µm), (b) An electrode in a jig that uses a spacer to enable the electrode cover-plate separation to be varied (in this case the spacer thickness is 125 µm). This is the jig and electrode system used for all the following measurements.

potential the WE potential is set against and is a platinum electrode surrounding the working electrode in a U-shape. The counter electrode is a large platinum electrode to the side of the reference electrode and supplies the current required at the working electrode to drive the electrochemical reaction.

Two key advantages of these electrode design choices are that:

- the location and dimensions of every nanoelectrode in the array, as well as the counter and reference electrodes are set by the design and accurately controlled;
- the chip design makes it straightforward to integrate all platinum electrodes making up the electrochemical three-electrode cell.

C. *Surface Tension Controlled Microfluidics*

The design of the liquid delivery system is based upon the approach described in reference [5]. It uses a hydrophobic pattern on a substrate to confine the liquid between it and another parallel plate, in this case a glass slide, and uses capillary action to fill the virtual well. In this work, Parylene C™ is used as the hydrophobic layer. The layout of the hydrophobic coating that creates the cell and electrode layout for the cell are documented in Fig. 2(b).

The test solution can be introduced into the cell either by:

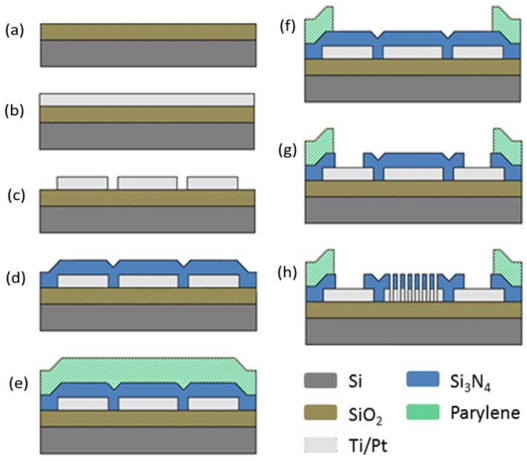

Fig. 4. The process flow for device fabrication (not to scale). (a) Growth of a layer of thermal SiO_2 on a Si wafer, (b) Deposition of a thin layer of Pt on a Ti seed layer, (c) Photolithographic patterning of the electrodes and contacts using reactive ion etching (RIE), (d) Deposition of silicon nitride, (e) Deposition of Parylene C™ (f) Patterning of Parylene C™ on top of the three electrodes to form the hydrophilic chamber area, (g) Patterning of the silicon nitride on top of the reference and counter electrodes (h) Etch of the silicon nitride and Ti/Pt layers to create the nanoelectrode array.

- Pipetting liquid into the hydrophilic channel close to the edge of the cover-glass above the electrode, which uses capillary action to fill the cell as detailed by Li et al. [6]; or
- Directly pipetting a known quantity of liquid onto the hydrophilic area where the electrodes are located and then completing the cell assembly by placing the spacer and cover glass over the liquid sample.

Either approach enables a set volume of liquid to be introduced into the cell with a pre-defined height. As detailed later, this control of both electrolyte volume and the height of the cover glass proves to be very beneficial when undertaking quantitative analysis.

D. Test Structure Chip Layout

The layout of the test structure chip (Fig. 2 (b)) consists of a hydrophilic cell area, surrounded by a patterned hydrophobic region, defining the electrolyte confinement area. The cell area contains the two platinum macroelectrodes (RE, CE) and the array of nanoelectrodes (WE). For the measurements reported in this paper, the array is made up of 1,536 square cavities of 30 µm side length arranged in a Cartesian grid with 120 µm pitch. This allows the characterization of the response on nano, micro and macro length scales at short, intermediate and long timescales [3]. It has been shown that nanoelectrodes can make measurements of kinetic parameters at short timescales, too fast to measure with larger electrodes. At intermediate timescales, a quantitative steady-state mass transfer limited current is established at each array element. For long timescales, the array behaves like a macroelectrode with an area equivalent to the total array footprint, but with reduced noise compared to a standard macroelectrode [4,7,8].

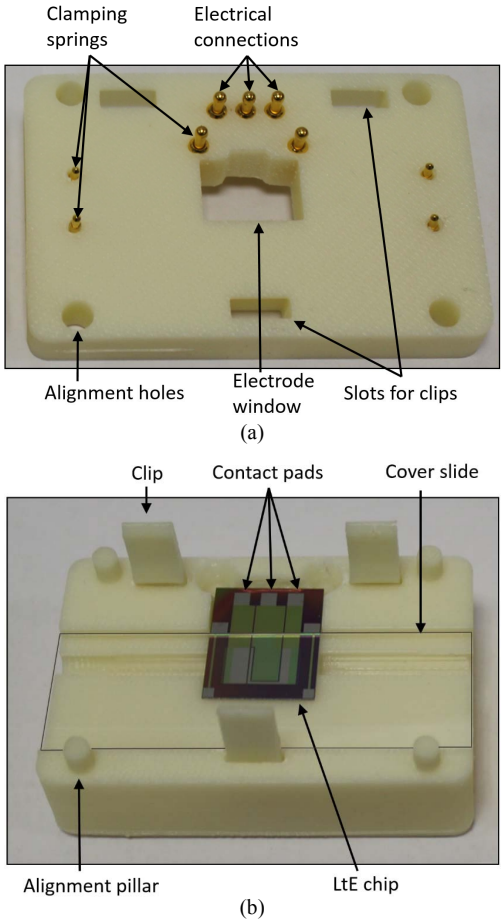

Fig. 5. Photographs of the unassembled components of the jig that positions the electrodes, spacer slide and cover-glass. (a) The top half of the 3D printed jig (underside), (b) the bottom half of the 3D printed jig (grey lines were drawn around the cover slide perimeter to improve clarity).

E. Fabrication of the Test Structure Chip

The fabrication for the electrodes is based on a process previously reported in [9] shown in Fig. 4. They were manufactured on 100 mm <100> n-type silicon wafers and the first process step is to thermally grow a 500 nm thick layer of silicon dioxide (SiO_2) to insulate the silicon from the electrode metal (Fig. 4(a)). Next, a 50 nm thick layer of platinum (Pt) is electron-beam evaporated onto the substrate following a 10 nm titanium (Ti) seed layer to aid adhesion (Fig. 4(b)). This titanium layer is not part of the final electrode dimension since it readily oxidizes to TiO_2 and becomes part of the insulating layer. Next, this metal layer is patterned to define the three electrodes, as well as their interconnects and contact pads (Fig. 4(c)). Following this, a 500 nm thick layer of silicon-rich silicon nitride ($Si_{3.1}N_{3.9}$) is deposited using low pressure chemical vapor deposition (Fig. 4(d)) and a final layer of 1000 nm of Parylene C™ deposited using a room-temperature polymerization process (Fig. 4(e)). The Parylene C™ covering the three bond pads and the fluidic chamber is then etched away using standard photolithography and an oxygen plasma (Fig. 4(f)). This is followed by the patterning of the silicon nitride layer using a CF_4/Ar etch to provide access to the bond pads, and form the reference and counter electrodes (Fig. 4(g)). Next, the nanoelectrode array is created by etching through both the silicon nitride and the

underlying Ti/Pt layers using a series of CF_4/Ar and Ar plasma etches (Fig. 4(h)). Finally, the wafers are diced into individual chips and treated with dilute tetramethylammonium hydroxide (TMAH) to ensure that the silicon nitride, silicon dioxide and platinum surfaces are hydrophilic and that the Parylene C™ is hydrophobic. The TMAH treatment results in an –OH termination of the silicon nitride, which makes it hydrophilic.

F. Cell Design

The system employs a 3D printed jig enabling the arrangement of the chip, spacer and cover glass. It consists of two sections that are connected using an integrated clip system and aligned using physical alignment features. The bottom part of the jig contains the moulds for the chip, cover glass and, if used, the spacer slide aligning them such that the contact pads are free to be connected to the electrical measurement equipment (Fig. 5 (b)). The cell height and thus liquid volume is set by the spacer thickness or features in the 3D printed jig and can be changed by selecting an appropriate spacer or jig.

The top section of the jig contains sprung gold pins to connect to the bond pads and hold all system components in place, as well as a liquid inlet, and a viewing window for visual inspection of the electrode area (Fig. 5 (a)).

The cell is assembled by locating the silicon test chip, spacer and cover glass into their respective recesses in the bottom section of the jig (Fig. 5 (b)) followed by clipping the top section (Fig. 5(a)) in place. Once the cell is fixed in position, the electrical connections are established via the sprung probes connected to the potentiostat, which completes the cell in readiness for performing electrochemical analysis.

III. Characterisation

A. Surface Layer wetting properties

Before use, dilute 2.3 % tetramethylammonium hydroxide (TMAH) was used to remove any surface contaminants and pre-treat the device surfaces. Table 1 presents the measured contact angles on the different surfaces of the test structure chip before and after 105 minutes of TMAH immersion.

TABLE I. Table Styles

Material	**Contact Angle**	
	Pre-TMAH	***Post-TMAH***
platinum	52˚ ± 12˚	40˚ ± 6˚
silicon nitride	36˚ ± 7˚	16˚ ± 4˚
array	34˚ ± 7˚	21˚ ± 7˚
Parylene C™	77˚ ± 8˚	87˚ ± 4˚

The results suggests the TMAH treatment lowers the contact of angle of a hydrophilic surface and increases the contact angle of a hydrophobic surface, while also decreasing the variability across the surface. A clear difference in contact angle was found between the Parylene C™ surface forming the hydrophobic pattern on the chip and the surfaces forming the hydrophilic chamber. Most importantly, the resulting Parylene C™ surface was found to have a mean increased contact angle of 87˚, which is close to the 89˚ measured by Li et al. [6]. This is worth noting because this earlier work only involved patterning Parylene C™

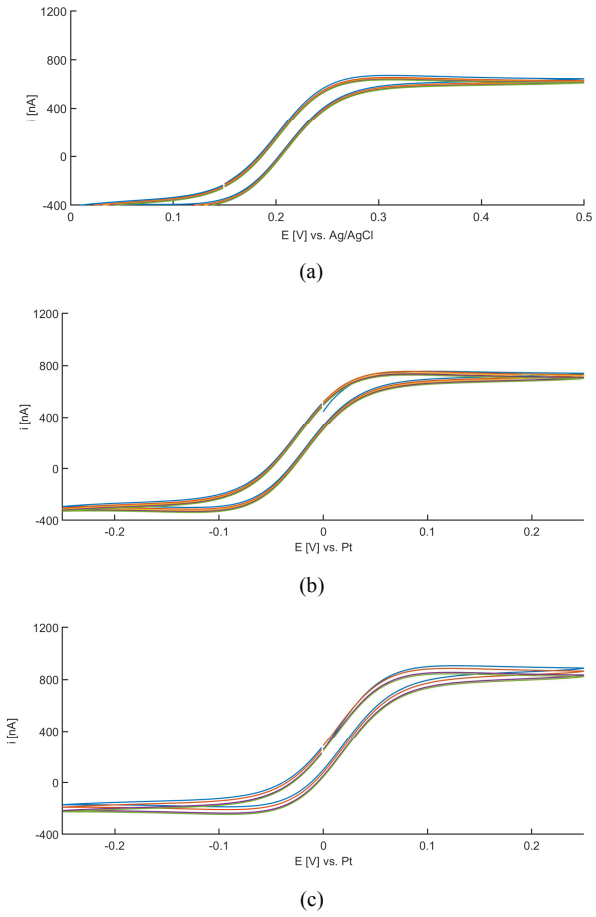

Fig. 6. Cyclic voltammograms showing the redox reaction of 250 µM ferrocenemethanol in 500 mM KCl for a scan rate of 0.1 Vs^{-1} using the on-chip nanoelectrode array (a) in a beaker with external electrodes (b) in a beaker using the on-chip counter and pseudo-reference electrodes (c) in the jig using the on-chip counter and pseudo-reference electrodes. Each colour represents a successive CV scan (first to fifth).

on silicon dioxide, so it is satisfying to note that the hydrophobicity is maintained in spite of the additional lithography and etch steps used for the devices detailed in this work. The surfaces exposed in the hydrophilic chamber area of the chip all have significantly lower contact angles with platinum being the least hydrophilic at 40˚. The silicon nitride areas show especially high hydrophilicity, indicating TMAH-treated silicon nitride is a suitable alternative hydrophilic surface to the previously used thermal SiO_2 [6].

The difference in contact angle between hydrophilic and hydrophobic elements was found to be sufficient to contain the liquid, as evidenced by the photographs shown in Fig. 3(a) and (b). However, should a larger difference in contact angle be required, Zou et al. detail a simple method of increasing the contact angle of Parylene C™ using plasma treatment of the surfaces [10]. Alternatively, more hydrophobic materials such as Teflon-AF™, or CYTOP™, can be used, the contact angles of which have been measured as 120˚ and 114˚, respectively [6].

B. Electrochemical Characterisation

The electroanalytical response of the test structure is measured using voltammetric and amperometric detection of the

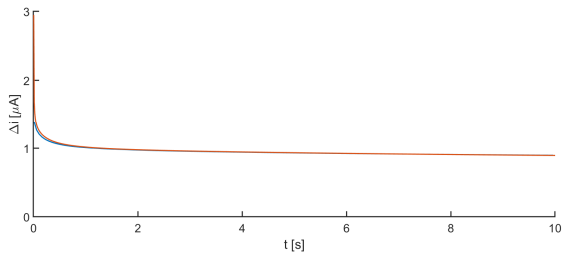

Fig. 7. Chronoamperometry recorded with configurations (i) (blue) and (iii) (red) for potential steps from the lower to the higher potential limit of the cyclic voltammograms in Fig. 6(a) and (c) (from 0 V to +0.5 V and -0.25 V to +0.25 V, respectively). The plotted current is the difference between the measured reductive and oxidative currents measured before and after the potential step.

oxidation reaction of a common redox couple, 250 µM ferrocene methanol (FcMeOH), in a test solution of 500 mM potassium chloride (KCl) background electrolyte. Before these measurements, all three on-chip electrodes were electrochemically cleaned by cycling between the oxidative and reductive solvent limits. The system was tested in three configurations:

- in a standard beaker assembly, using the on-chip nanoarray as the working electrode and external, commercial counter and reference electrodes,
- in a standard beaker assembly, using the three on-chip electrodes, and
- in the thin layer cell configuration with a liquid height of 125 µm.

A cyclic voltammogram (CV) with external counter and reference electrode showed the previously established response of the nanoarray (Fig. 6 (a)) [4,7,8]. This was followed by testing the response of the complete test chip in a beaker (Fig. 6 (b)), and, finally, in the fully assembled small volume thin layer cell configuration (Fig. 6 (c)).

All three configurations show a similar electrochemical response with comparable current magnitudes. The potential limits and scan rate (100 mVs^{-1}) were chosen to give a cycle time of 10 s and a net oxidation of FcMeOH in each cycle. The characteristic diffusion lengths, l_{diff}, of half the pitch, the chamber height and the distance between array edge and RE were 60 µm, 125 µm and 350 µm, respectively. The resultant characteristic diffusion times, l_{diff}^2/D, were estimated as 7 s, 30 s and 250 s for a typical diffusion coefficient of FcMeOH of 5 x 10^{-10} m^2s^{-1}. The first of these times confirms why the array is observed to give a near steady state response from each electrode, as in each cycle the diffusion length has not grown sufficiently for significant diffusion layer overlap with neighboring electrodes. The second time indicates why the currents change with successive cycles in the thin layer cell due to product accumulation close to the electrodes. This product accumulation can be used e.g. to analyze samples that are difficult to obtain or instable in their oxidized or reduced state.

Switching from an external Ag/AgCl RE (Fig. 6 (a)) to an on-chip platinum pseudo-RE (Fig. 6 (b)) produces the expected change in observed redox potential to near 0 V, consistent with the redox couple determining the reference potential. This reference potential corresponds to the reduced end of the redox couple, indicating that, as expected, only a very small amount of oxidized FcMeOH is initially present at the reference electrode surface. When comparing the in-beaker (Fig. 6 (b)) and test chip cell (Fig. 6 (c)) there is a small offset in potential intercept of a few mV, as can be expected in different experiments using a pseudo-RE.

These characteristics are confirmed using potential step experiments (Fig. 7) which show no difference in measured current in the beaker and thin layer cell configuration, as well as an unchanging current for the duration of the measurement.

IV. Conclusions

This paper has outlined details of a test structure and measurement system together with the quantitative analytical benefits of integrating a number of technologies to create a cell for electrochemical characterization in which the electrolyte volume can be set. The paper also confirms that the quantitative test chip characterization data at least matches, and in some aspects surpasses, conventional in-beaker measurements. In particular, it provides the opportunity to characterize the electrochemical response using solutions that are expensive or difficult to obtain in large volumes, as well as providing more rapid characterization of bulk solutions. The significant improvements in ease of use over beaker measurements include:

- reduced and controlled sample volume, ideal for expensive or hazardous analytes;
- robust and simple disassembly and reassembly for easy and rapid cleaning;
- precise control of the electrode placement and spacing;
- a gasket- and seal-free microliter volume cell;
- small liquid volume simplifying sample temperature control;
- fixed electrical contacts that avoid potential shorting or degradation of connections; and
- when using this type of nanoelectrode array, a comparable response of the thin film cell configuration and a beaker is measured.

The small, but known, volume and geometry of the cell also enables the fast and quantitative electrochemical conversion of a species for subsequent analysis using either electrochemical or optical techniques. Overall, the results demonstrate the nano array test chip to be a very versatile architecture for rapid quantitative electroanalytical studies.

Acknowledgments

We would like to thank Dr. Tom Barraclough, Markus Nemitz and Constantine Talalaev (University of Edinburgh) for support with aspects of jig and spacers fabrication. We also acknowledge funding through the EPSRC under EP/J000779/1 and EP/L018616/1 (EB, IS) and the European Commission under FP7 323282 (IS). Data is available from http://hdl.handle.net/10283/2769.

REFERENCES

[1] J. Heinze, "Ultramicroelectrodes in electrochemistry," Angew. Chem. Int. Ed. Engl., vol. 32, pp.1268-1288, 1993.

[2] C. Amatore, C. Pebay, L. Thouin, A. Wang and J.-S. Warkocz, "Difference between ultramicroelectrodes and microelectrodes: influence of natural convection,"Anal. Chem., vol. 82, 6933-6939, 2010.

[3] J.T. Cox and B. Zhang, "Nanoelectrodes: recent advances and new directions," Annu. Rev. Anal. Chem., vol. 5, 253-272, 2012.

[4] I. Schmueser, A.J. Walton, J.G. Terry, H.L. Woodvine, N.J. Freeman, A.R. Mount, "A systematic study of the influence of nanoelectrode dimensions on electrode performance and the implications for electroanalysis and sensing," vol. 164, 295-314, 2013.

[5] E.O. Blair, L. Parga Basanta, I.Schmueser, J.R.K. Marland, A. Buchoux, A. Tsiamis, C. Dunare, M. Normand, A.A. Stokes, A.J. Walton and S. Smith, "Wafer Level Characteriation of Microelectrodes for Electrochemical Sensing Applications," Proc. IEEE International Conference on Microelectronics Test Structures 2018, 9-2

[6] Y. Li, E.O. McKenna, W. Parkes, A.R. Pitt and A.J. Walton, "The application of fixed hydrophobic patterns for confinement of aqueous solutions inproteomic microarrays,"Appl. Phys. Lett., vol. 99, 073703-1-073703-3, 2011.

[7] N.J. Freeman, R. Sultana, N. Reza, H.L. Woodvine, J.G. Terry, A.J. Walton, C.L. Brady, I. Schmueser, A.R. Mount, "Comparison of the performance of an array of nanoband electrodes with a macro electrode with similar overall area,"Phys. Chem. Chem. Phys., vol. 15, 8112-8118, 2013.

[8] R. Sultana, N. Reza, N.J. Kay, I. Schmueser, A.J. Walton, J.G. Terry, A.R. Mount, N.J. Freeman, "Practical implications of using nanoelectrodes for bioanalytical measurements," Electrochim. Acta., vol. 126, 98-103, 2014.

[9] J.G. Terry, I. Schmueser, I. Underwood, D.K. Corrigan, N.J. Freeman, A.S. Bunting, A.R. Mount, A.J. Walton, "Nanoscale electrode arrays produced with microscale lithographic techniques for use in biomedical sensing applications," IET Nanobiotechnol., vol. 7, 125-134, 2013.

[10] H. Zou, Y. Li, S. Smith, A.S. Bunting, A.J. Walton and J.G. Terry, "Modification and characterisation of material hydrophobicity for surface acoustic wave driven microfluidics," IEEE Proc. Int. Can! Microelectronic Test Structures (ICMTS), 2012.